VSS 2025
#36.327

Modeling the statistical properties of natural images and medical radiographs

Vicky Cai[1] and Jonathan Victor[2]
[1]Stuyvesant High School, [2]Weill Cornell Medical College, New York, NY, USA

INTRODUCTION

- Many aspects of human vision are tuned to the characteristics of its natural inputs, including global statistics (power spectrum) and local statistics (multipoint correlations)
- Medical radiographs have a steeper spectral slope and a different pattern of local statistics.
- Natural images and radiographs are formed by different physical processes. As a consequence, occlusion is typical in natural images; transparency is typical in radiographs.
- However, the role of these differences (as well as others) in shaping image statistics is unclear.

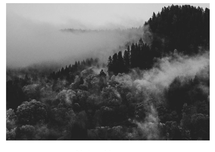
Natural image


X-ray image

STRATEGY

To investigate the basis of differences in image statistics between natural images and radiographs, we built simple generative models and compared their statistics. Generative models differed in:

- Occlusion vs. transparency
- Dimensionality (2D vs 3D objects)
- Object size distribution

IMAGE PROPERTIES EXPLORED

1) **Occlusion vs. transparency:** We used the dead leaves model (Ruderman 1997) to model occlusion and a variation (Zylberberg, 2012) to model transparency.
2) **Dimensionality**: We generated scenes with 2D objects (circles) and 3D objects (spheres), randomly positioned.
3) **Size distribution:** Radii were drawn from a power-law distribution $p(r)=kr^{-\alpha}$, within a range. We examined α=1, 2, or 3.

References

Ajayi, E., and Victor, J.D., (2023) Statistical characterization of medical images of bone. (Abstract) Vision Sciences Society Annual Meeting, St. Petersburg, FL, Journal of Vision 2023; 23(9): 4698. doi:doi.org/10.1167/jov.23.9.4698

Hermundstad, A.H., Briguglio, J.J., Conte, M.M, Victor, J.D., Balasubramanian, V., and Tkačik, G., (2014) Variance predicts salience in central sensory processing. eLife 2014;10.7554/eLife.03722.

Ruderman, D.L. (1997) Origins of scaling in natural images. Vision Res. 37(23):3385-98. doi: 10.1016/s0042-6989(97)00008-4.

Tkačik, G., Ratliff, C.P., Milčinski, G., Klein, J.M., Seyfarth, L.H., Sterling, Pl, Brainard, D.H., and Balasubramanian, V. (2011) Natural images from the birthplace of the human eye," PLoS One, vol. 6, no. 6, p. e20409

Victor, J.D., and Conte, M.M. (2012) Local image statistics: maximum-entropy constructions and perceptual salience. Journal of the Optical Society of America A, 29, 1313-1345.

Xu, Y., Raj, A., and Victor, J.D. for the Alzheimer's Disease Neuroimaging Initiative (2019) Systematic differences between perceptually-relevant image statistics of brain MRI and natural images. Front. Neuroinform. 13:46. doi: 10.3389/fninf.2019.00046.

Zylberberg J., Pfau D., DeWeese, M.R. (2012) Dead leaves and the dirty ground: Low-level image statistics in transmissive and occlusive imaging environments. Phys Rev E Stat Nonlin Soft Matter Phys. 86(6 Pt 2):066112.

METHODS: GENERATIVE MODELS

All images were created using Python (OpenCV and Numpy libraries) and Java.

Occlusion Models

2D (OC2)
We used the standard dead leaves model (Ruderman, 1997), with reflectances of each object drawn uniformly from [0,1].

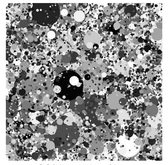
OC2 Image (α = 2)

3D (OC3)
Spherical objects were rendered using Lambertian reflectance and orthogonal projection, with each object's reflectance drawn uniformly from [0,1]. The illuminant was located behind the viewer.

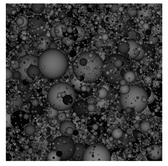
OC3 Image (α = 2)

Transparency Models

2D (TP2)
For the regions of overlap between circles, the transparency is the product of the transparencies of the overlapping circles. The image contrast was inverted after adding all circles. Transparencies were drawn uniformly from [0,1].

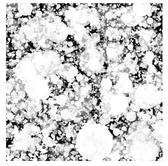
TP2 Image (α = 2)

3D (TP3)
The Beer-Lambert Law was used to calculate the intensity at each pixel, based on the path length through the spheres. Density was drawn uniformly from [0,1]. Thickness was calculated by finding the length of the chord in the sphere from each point.

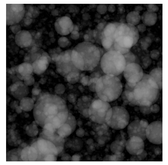
TP3 Image (α = 2)

Other model parameters

- **Image size:** all images were 512 x 512 pixels
- **Object size limits:** Radii were restricted to a range of 2 to 64 pixels
- **Coverage**: The number of objects was chosen so that each point in the image was covered by an average of 3 objects.
- **Number of examples:** 500 examples of each image class were generated for statistical analysis.

METHODS: IMAGE ANALYSIS

All analyses were carried out using Python (Matplotlib)

Power Spectra

- Each image was windowed with a Gaussian
- The Fourier transform was taken and the amplitudes were squared
- Average squared amplitudes were computed across the image set
- Spectral slope was computed after radial averaging, by regression for frequencies in the range $[N/(2\ r_{max}), N/(2\ r_{min})]$

Multipoint Correlations

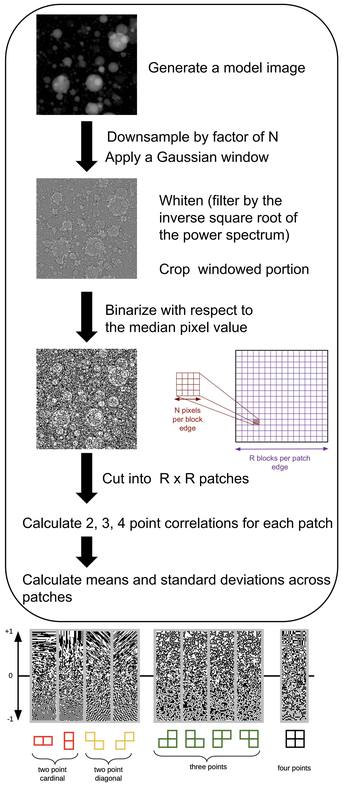

Each multipoint correlation is an independent measure of local statistical structure, and can range from -1 to 1.

RESULTS

Global Statistics

Power spectra

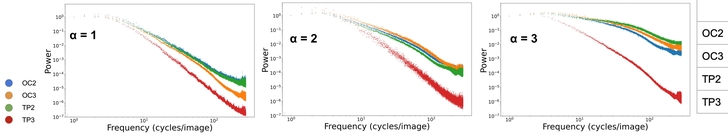

Spectral slopes

	α = 1	α = 2	α = 3
OC2	−2.71	−2.00	−1.36
OC3	−2.96	−2.00	−1.18
TP2	−2.75	−2.19	−0.86
TP3	−3.74	−3.60	−3.01

- Three of the models (OC2, OC3, TP2) had spectral slopes similar to that of natural images (~-2), for α=2.
- The steeper spectral slope of radiographs (~-2.7 to -3) was captured by TP2 (for α=1), and for TP3, for all values of α

Local Statistics

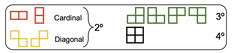

Generative models

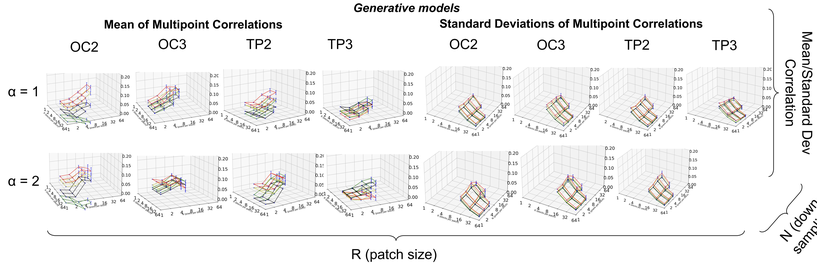

Natural Images
(Penn Natural Image Database)

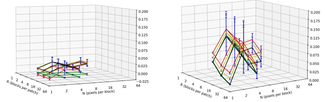

Bone Radiographs (Ajayi, VSS 2023)

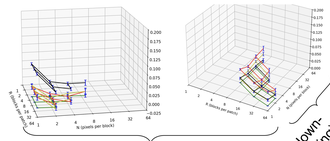

Mean correlations – represent overall characteristics of each image set

- The pattern of mean values of the correlations depended on all aspects of the model: occlusion vs. transparency, dimensionality, and size distribution.
- For all variants of the occlusion model, the mean value of the cardinal second-order statistic was the highest.
- In the TP models, the mean correlations depended on size distribution: correlations for α = 2 were higher than for α = 1.

Comparison with natural images and radiographs

- In natural images, 4-point correlations have the highest mean, followed by 2-point cardinal, diagonal, and 3-point, In bone radiographs, 4 pt correlations have the highest mean, followed by approximately the same means for 2-point cardinal, 2-point diagonal, and 3-point correlations (Ajayi et al., 2023)
- None of our models could account for the pattern seen in natural images or in radiographs: in our model image sets only TP3 for α = 1 accounted for the high 4-point correlation, but it failed to account for the lower order correlations.

Standard deviations of correlations – represent the patch-to-patch differences in statistics and what is needed discriminate among images within a set

- Standard deviations had a similar ordering for all models.
- Standard deviations had a similar dependence on scale (N and R) for all models.
- The 2-point cardinal standard deviation was slightly higher than the others in most models, and there was little separation between 2-point diagonal, 3-point, and 4-point correlations.

Comparison with natural images and radiographs

- In natural images, 2-point cardinal correlations have the largest standard deviation, followed by 2-point diagonal, 4-point, and 3-point, corresponding to human visual sensitivity (Hermundstad et al., 2014; Victor and Conte 2012).
- In bone radiographs, 2-point cardinal correlations have the largest standard deviation. 2-point diagonal and 4-point are about the same, and 3-point is the smallest.
- None of our models could account for the standard deviations of correlation seen in natural images or radiographs.

SUMMARY AND CONCLUSIONS

- Global statistics: occlusion models could account for the power spectrum of natural images and transparency models could account for the power spectrum of radiographs.
- Local statistics: The method of image formation had a large effect on the mean values of local image statistics, but a more subtle effect on their standard deviations.
- Local statistics: The models could not account for the patterns of either the mean values or the standard deviations of correlations in natural images and radiographs.

NEXT STEPS

- Wider variety of shapes (more organic)
- More realistic generative models (ray tracing)

Support: NIH NEI 07977